

Seismic Behavior of Self-centering Designed Eccentrically Braced Frames

Chin-Tung Cheng & Chih-Hong Hsu

National Kaohsiung First University of Science and Technology, Taiwan

Ker-Chun Lin

National Center for Research on Earthquake Engineering, Taiwan



SUMMARY: (10 pt)

It is well known that seismic energy is dissipated through the plastic deformation of link beam in the Eccentrically Braced Frames (EBF). However, large residual deformation after earthquakes makes the structure difficult to repair. Therefore, this paper investigates the feasibility of applying a self-centering function on the link beam of EBF to reduce the residual deformation after the earthquakes. Unlike literatures separated beam-column interfaces so that beams rocked on column faces without damage incurred during earthquakes. In this research, the rocking interface is relocated to the interface of link beam and adjacent beams in EBF. Due to the frame geometry, opening at the interface on EBF may be amplified from the interstory drift, resulting in better efficiency in energy dissipation by dampers installed at this interface, therefore, enhances the seismic performance of the EBF.

Keywords: Eccentrically Braced Frame, Self-centering, Link Beam, Frictional Hinge Damper

1. GENERAL INSTRUCTIONS

In tradition, seismic energy is dissipated through the plastic deformation of link beam in the Eccentrically Braced Frames (EBF). However, large amount of residual deformation results in difficulties in repairing the structure after earthquakes. Therefore, this paper investigates the feasibility of applying the self-centering function in the link beam of EBF in order to avoid the damage due to earthquakes. Regarding the research of self-centering function in structures, Mander and Cheng [1] have proposed a seismic design concept referred to as Damage Avoidance Design for bridge piers in 1997. In 2002, Christopoulos et al. [2] investigated the feasibility of self-centering function applied for the steel structures, using post-tensioned strands to connect beams and columns. Test results showed that connections did have self-centering function. And provided buckling restrained high strength bar showed enough energy dissipation capacity, however, its fan shape hysteretic loop had less energy dissipation capacity than the traditional one with elasto-plastic hysteretic loop. Similar research was done by Ricles et al. [3] in 2002, steel angles were applied to dissipate energy in concrete-filled steel tubular connections. In 2008, Tsai et al. [4] and Wolski et al. [5] used friction force to dissipate seismic energy in self-centering steel structures.

Unlike above-mentioned literatures that separated the beam on column faces (rocking interface) to release its high plastic strain demand at the beam end, in this research, separation is relocated to the interface of central link beam and the adjacent beams of EBF, accompanied with post-tensioned tendons that connected the beams and column to achieve the self-centering function. The advantage of this relocation is to amplify the opening at this interface from the interstory drift due to the frame geometry, when the structure is subjected to lateral loads. This amplification results in larger relative displacement between both sides of interface as well as better efficiency of energy dissipation by dampers installed at the interface, therefore, enhances the seismic performance of the EBF.

2. SPECIMENS AND TEST PROCEDURES

To validate the proposed idea, a full-size one storey-one span EBF was constructed and tested under lateral cyclic reversed loads. The specimen has a 2m long central link beam with two braces. The height and span of frame are 3.2m and 5.15m respectively. The cross-section of columns, link beam and adjacent beams is $400 \times 400 \times 13 \times 21 \text{mm}$, $400 \times 200 \times 8 \times 13 \text{mm}$ and $600 \times 200 \times 11 \times 17 \text{mm}$ in size, respectively. Beams welded to the end plate were connected to column by bolts and then post-tensioned by two seven wire prestress strands (DSI 6807 G270) at the beam web. Bottom columns welded to an end plate were connected to a rotational-free hinge by bolts, which were seated on the strong floor. Two braces $150 \times 150 \times 7 \times 10 \text{mm}$ in size were fillet welds to the gusset plates to connect with beams and columns, respectively. For erection purpose, central link beam was seated on steel angles bolted to the end plate of adjacent beams. Before the test, bolts on the link beam were temporarily removed so that link beam could freely rock on the end plate of adjacent beams during tests.

To enhance the seismic performance of the self-centering EBF, frictional hinge dampers or steel angles were applied to increase the energy dissipation of the specimen. As shown in **Figure 1**, one frictional hinge damper was installed on the each side of adjacent beam webs, totally eight dampers for one central link beam. Each damper is consisted of four 20mm thick 150mm diameter circular brass plates sandwiched with 20mm thick steel plates and the beam web, all bolted together by a high strength threaded bar. When the rocking interface between link beam and adjacent beam starts to open, a rectangular bar will pull the sandwiched steel plate to rotate against the brass plates, resulting in friction energy that may vary with the prestress applied on the high strength threaded bar. Another type of energy dissipation is using the steel angles on which link beam have seated. In total, four steel angles were installed on one central beam. Due to the limitation of beam depth, two sizes of steel angles $75 \times 75 \times 9 \text{mm}$ and $100 \times 100 \times 13 \text{mm}$ all have 110mm length were applied. Each angle was anchored by using two M22 A325 bolts on each leg, as shown in **Figure 1**.



Figure 1. Left photo shows the frictional hinge damper and right photo shows steel angles installed

Investigation parameters include types of energy dissipation device such as frictional hinge dampers or steel angle, various clamping force on the dampers and size of steel angles. As shown in **Table 1**, totally five tests were conducted. In the test numbering, first character F or A means frictional hinge dampers or steel angles were installed. The second character 0, 20, and 25 indicates zero, 200 kN and 250 kN clamping force applied on the dampers, respectively. And 9 and 13 means 9 mm or 13 mm thick steel angles applied to dissipate energy. M_P in **Table 1** shows the plastic strength of the link beam, and M_{pti} indicates the post-tensioned moment achieved by applying 260 kN prestress on each DSI6807 tendon. The ratio of M_{pti} / M_P should be higher enough to let the frame re-centering after unloading, while it should be lower enough so that the post-tensioned strands will not be yielded when the frame reached its target drift such as 0.02 rad in this design. M_{ED} is the moment provided by energy dissipater at the target drift, while M_D is the moment required to open

the rocking interface. The last column in **Table 1** shows the stress ratio of post-tensioned strands with respect to its yielding strength at the target drift. It is found that this ratio is far less than 1, which means the stress of post-tensioned strands will remain elastic at all time during tests.

Table 1 Tested parameters

Tests	M_{pl}/M_p	M_{ED}/M_p	M_D/M_p	$M_{0.02}/M_p$	$F_{pl0.02}/F_{PTY}$
F0	0.21	0.00	0.21	0.61	0.63
F20	0.21	0.07	0.28	0.67	0.63
F25	0.21	0.08	0.30	0.69	0.63
A9	0.21	0.14	0.21	0.76	0.63
A13	0.21	0.23	0.21	0.94	0.63

Figure 2 shows the test setup. A 1000 kN actuator applied cyclic reversed horizontal load with displacement control in the form of triangular waves. The displacement cycles consisted of 6 cycles of 0.25%, 0.5% 0.75%, 4 cycles 1%, and 2 cycles of 1.5% and 2.0% storey drift. The displacement rate for all cycles was set to be constant as 1mm/sec. Two 1000 kN load cells were used to monitor the force in two post-tensioned strands, while four 500 kN load cells measured the normal force applied on the frictional hinge dampers. Four LVDTs measured the opening at the interface of link beam and adjacent beams. Totally three lateral supports were applied, one at the central link beam and two at adjacent beams.

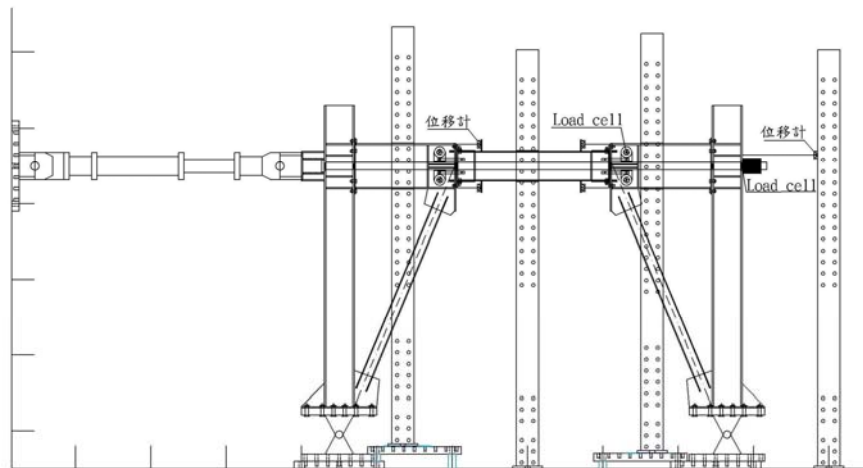


Figure 2. Test setup

3. TEST RESULTS

It was found that the frame remained elastic at all time without inducing damage after five successive tests. The tests applied with frictional hinge dampers were successively conducted by the increase of normal force on dampers; while the steel angles were renewed in each test since they were yielded or fractured during test. **Figure 3** shows the hysteretic loop of five tests. It can be seen that little energy was dissipated in each test. For the tests with frictional hinge dampers, strength of the first and successive cycles remains the same, while it is slightly deteriorated after the first cycle for the tests with steel angles. Visual observation reveals that out of plane rotation in central link beam became significant when the lateral displacement reached 1% drift for all tests. This out of plane rotation results from inappropriate test setup, resulting in less opening at the rocking interface and the increase of the friction force between the frame and lateral supports, especially when the frame is subjected to push loads. In the tests applied with steel angles as energy dissipater, the amount of out of plane rotation is found less than those in the tests applied with frictional hinge dampers due to the restraint

of steel angles at the separating interface.

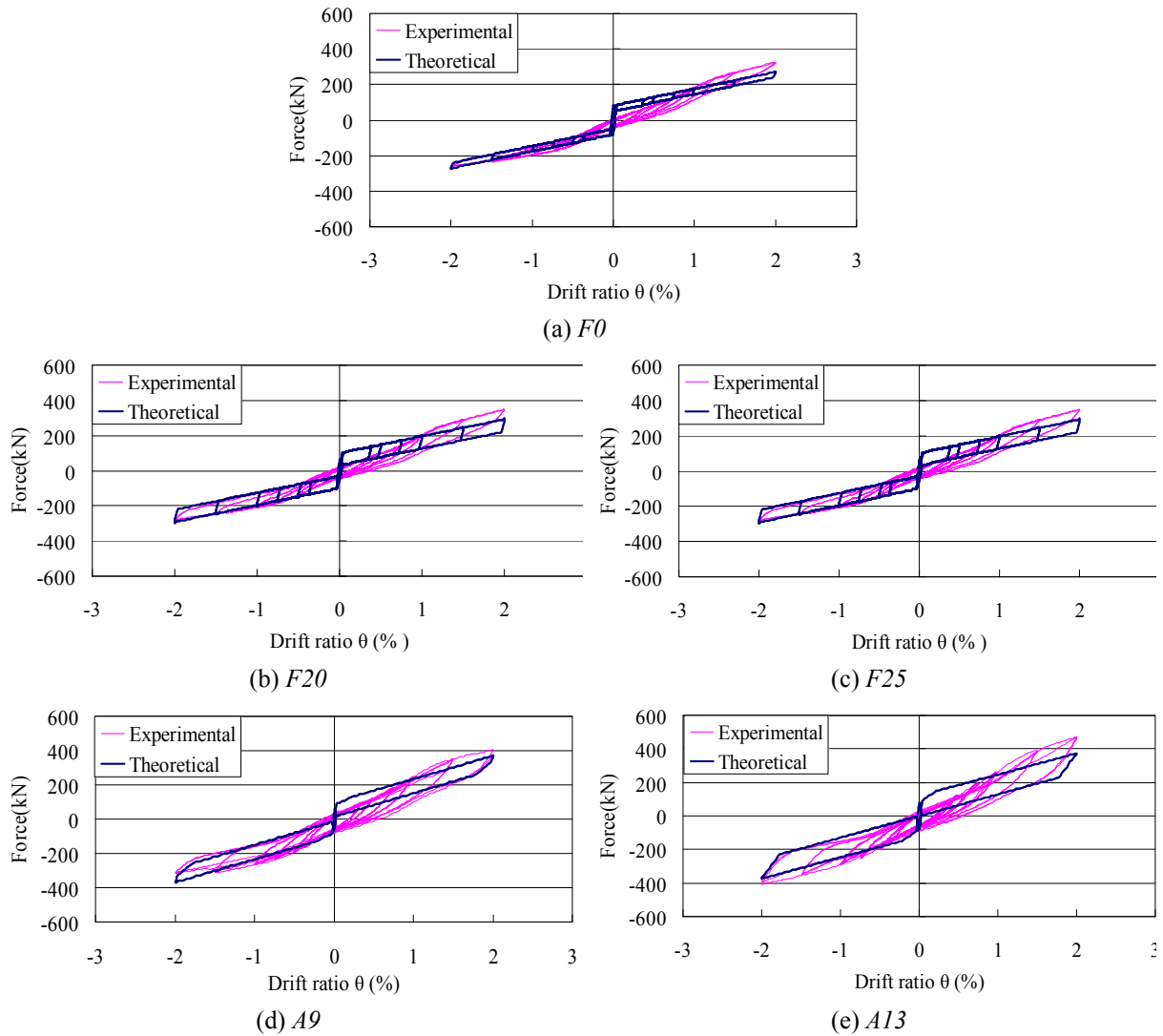


Figure 3. Hysteretic loop for the tests

The resisting force of the EBF frame can be decomposed into three components such as forces due to the prestress, dampers and the braces. If taking out the resisting force contributed by the braces, hysteretic loops as shown in **Figure 3** can be transformed into **Figure 4**. It can be seen that the self-centering designed EBF is indeed recentering after loads. And the frames applied with steel angles have larger energy dissipation capacity than those installed with frictional hinge dampers under current design.

As mentioned in the introduction, the opening in the interface between the central link beam and adjacent beams may be amplified from the storey drift. **Figure 5** shows the deformed relations of EBF before and after lateral loads based on its geometry. Rotation γ in link beam may be amplified from the storey drift ratio θ with the relation of $\gamma = \frac{L}{e}\theta$. Based on the realistic geometry in this test, the amplification ratio is calculated as 2.5. **Figure 6** illustrates the comparison of theoretical and measured openings at two interfaces along with the increase of storey drift for five tests. Among four scenarios in each test, it can be seen that right interface of the link beam, which is far from the loading application as illustrated in **Figure 5**, has less openings than the left interface. In addition, since less out of plane rotations observed in the tests under pull loads, its openings are closer to the theoretical

one and always larger than those applied with push loads.

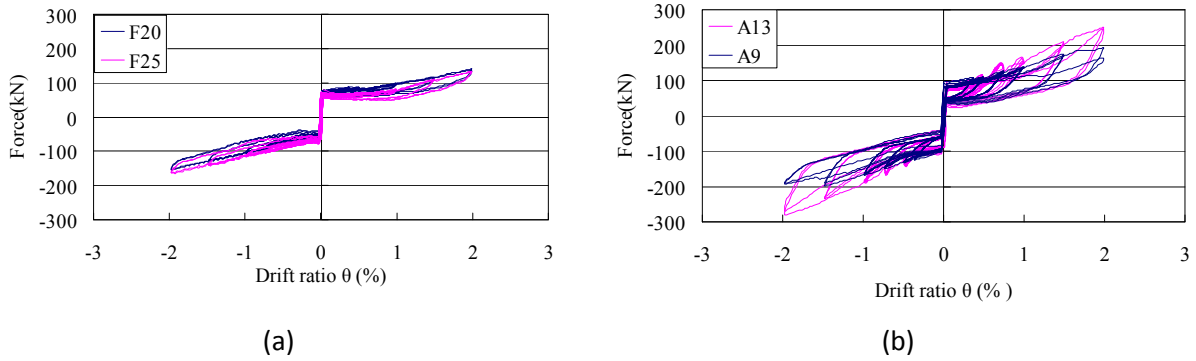


Figure 4. Force-deformation curves due to dampers and the prestress

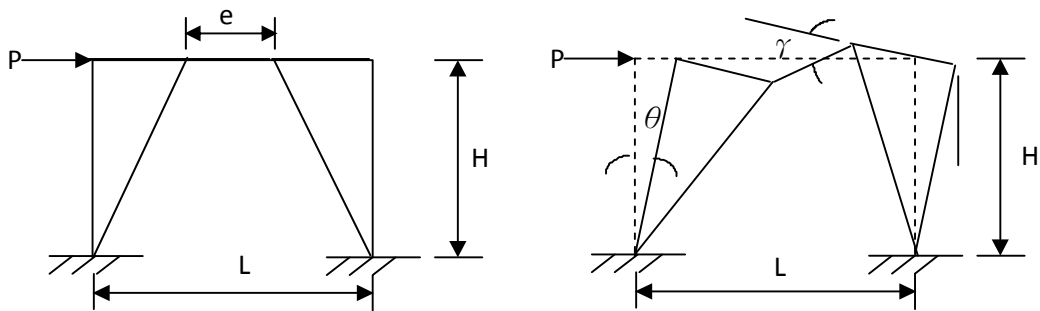


Figure 5. Relation between link rotation and storey drift

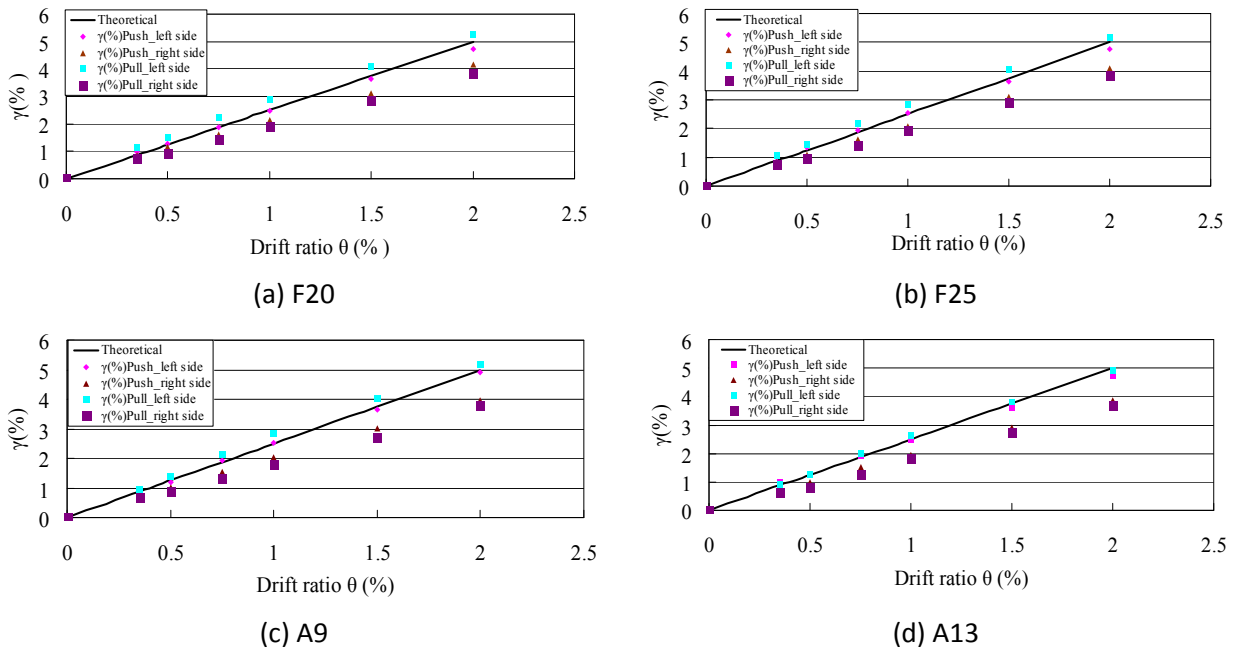


Figure 6. Theoretical and experimental opening at the interface

4. SIMULATIONS OF FORCE – DEFORMAION BEHAVIOR

Force-deformation relation of the frame can be decomposed into three components, such as stiffness

contributed from the brace, self-recentering function provided by post-tensioned tendons and energy dissipation by the FHDs or steel angles. Therefore, force-deformation behavior due to each component is sequentially simulated and then composed together.

4.1. Self-centering Mechanism

When the rocking interface is closed, the frame stiffness relies on axial stiffness of the braces and expressed as

$$K = \frac{E_s A_s}{L} \cos(\alpha)^2 \quad (1)$$

where α is the brace angle with respect to the horizontal, A_s is cross section of the brace, E_s is steel modulus, and L is the length of the brace. When the interface starts to open, link beam will rotate with respect to the top or bottom corner of the beam end and prestress tendons at the beam web will be elongated based on the geometry

$$\varepsilon_{PT} = \varepsilon_0 + \left[\frac{(d_b/2 - c) \cdot \gamma}{L_{PT}} \right] \left(1 - \frac{A_{PT}}{A_b} \right) \quad (2)$$

where ε_{PT} is the strain of post-tensioned tendons during testing, ε_0 is initial strain in the tendons before tests, d_b is the depth of the link beam, c is the depth of neutral axis on the link beam, L_{PT} is the anchorage length of the tendons, and A_{PT} and A_b are the cross sectional area of the tendons and link beam, respectively. The tendon force and moment can be respectively expressed as

$$F_{PT} = A_{PT} E_s \varepsilon_{PT} \quad (3)$$

And

$$M_{PT} = 2F_{PT} \left(\frac{d_b}{2} - c \right) \quad (4)$$

Sub-headings are printed in 11pt bold as shown. Use upper and lower case letters. Leave one blank line above a sub-heading and one blank line between sub-heading and the first line of the text.

4.2. Frictional Hinge Damper

To derive the energy dissipated by the frictional hinge damper, it is assumed that the normal force is uniformly distributed over the surface of circular brass plate. By dividing the area of brass plate into sub-area (ring), the torsional moment resisted by the friction damper can be calculated by cumulating the product of friction force in each ring and its distance, ρ , with respect to the center of the plate expressed as

$$T_f = \int_0^r \mu \frac{N}{\pi r^2} 2\pi \rho d\rho \cdot \rho = \frac{2\mu N r}{3} \quad (5)$$

Where N is the normal force applied on the damper, r is the diameter of the brass plate (75mm), μ is the friction coefficient between the steel plate and brass plates. Morgen and Kurama indicated that the friction coefficient was among 0.17~0.2. In this research, friction coefficient of 0.2 is assumed. The total resisting friction moment by the dampers is

$$F_f = T_f n_b n_f \quad (6)$$

Where n_f is number of friction surface (2 surfaces for each damper) and n_b is number of frictional hinge damper (8 dampers per link beam). The resisting moment with respect to the rocking toe of the link beam is expressed as

$$M_f = \frac{F_f}{h_f} \times \frac{d_b}{2} \quad (7)$$

Where h_f is the distance between the center of the damper and rectangular bar that pulls the steel plate to rotate (100 mm). As shown in **Figure 7**, total resisting moment is the superposition of the recentering moment due to post-tensioned strands and friction moment due to dampers as

$$M = M_{PT} + M_f \quad (8)$$

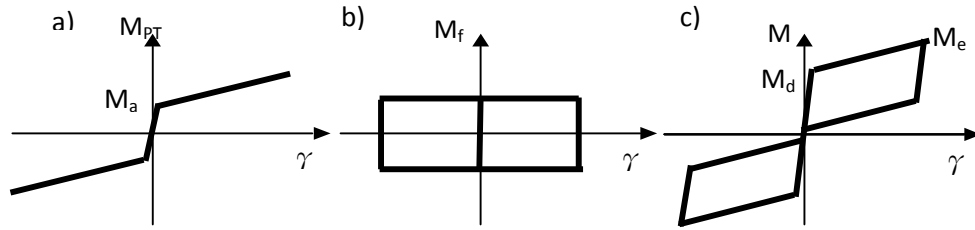


Figure 7. Self-centering EBF installed with frictional hinge damper

4.3. Steel Angle

The energy dissipated by the steel angles can be derived based on the research of Ricles et al. [3]. Accordingly, the resisting force, V_{AP} , by the steel angles is expressed as

$$V_{AP} = \beta V_p = \beta \times \frac{2M_{pa}}{g} \quad (9)$$

Where β is overstrength factor of the angles, V_p is material strength of the angles, M_{pa} is flexural strength of the angle and g is the gauge length from the edge of the bolts to the surface of the angle flange. Since angle size in this research is different with the literature, the relation of resisting force of the angles versus displacement in this research is obtained by firstly transforming the relation of literature into a stress-strain relation and then multiplying the size of this research to get the force-deformation relation. As shown in **Figure 8**, total resisting moment is the superposition of re-centering moment due to post-tensioned strands and material strength due to steel angles as

$$M = M_{PT} + M_{ag} = M_{PT} + 2V_{AP} \times d_b \quad (10)$$

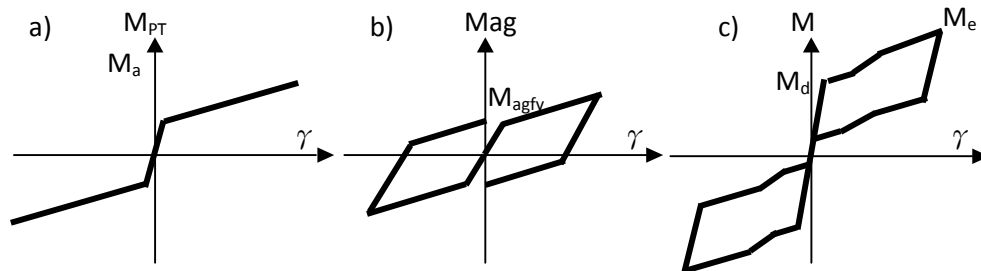


Figure 8. Self-centering EBF installed with steel angles

4.4. Comparison of analytical and test results

Figure 3 shows the comparison of experimental and analytical hysteretic loops. As shown in the figure, tested initial stiffness is far less than the theoretical one. This may result from existing void within the interface that was closed until applied with extensive loads, or slips occurred within the interface during loading. After the stage of initial loading, it is found that analytical strength agrees well with test results when subjected to pull loads, while predictions will be less than the tests under push loads, since significant out of plane rotation observed in the link beam increased the friction force between lateral supports and the frame.

5. CONCLUSIONS

On the basis of experimental and analytical results, following conclusions can be drawn:

- (1) The frame remained elastic and undamaged at all time during five successive tests. Post-tensioned strands provided self-centering function, even though minor residual displacements found after tests due to the friction force existed between the frame and lateral supports, resulting from out of plane rotation of the link beam.
- (2) Based on current design of this research, test results seem indicate that energy dissipation by the steel angles is better than that of the frictional hinge damper, while it can be enhanced by increasing the clamping force applied on the damper. It is also found that dampers remained undamaged, while fractured angles have to be replaced after tests. It is recommended that both energy dissipaters should be simultaneously applied on the frame to enhance the seismic performance of EBF.
- (3) Based on the comparison of analytical and experimental results, it is found that proposed analytical model could predict the force and displacement relations of the EBF. Due to the voids or slips existing within the interface, tested initial stiffness of the frame is far less than that of the analytical model. After that, it is found that lateral strength of the frame was increased under push loads, resulting from out of plane rotation observed in the link beam that increased the friction force between the frame and lateral supports.

ACKNOWLEDGEMENT

Financial supports from the National Center for the Research on Earthquake Engineering (NCREE) and National Science Council in Taiwan, with the grant NSC98-2625-M-327-003 are highly appreciated. The authors would also like to thank engineer in NCREE Mr. Chih-Hsiung Chou and An-Chih Chen for their assistance in experiments.

REFERENCES

- Christopoulos, C., Filiatraut, F., Uang, C-M. and Folz, B. (2002) Post-tensioned energy dissipating connections for moment resisting steel frames. *Journal of Structural Engineering, ASCE*, 128:9, 1111-1120.
- Mander J.B, Cheng C-T. (1997) Seismic resistance of bridge piers based on damage avoidance design. Technical Report *NCEER 97-0014*; Buffalo, NY.
- Morgen, B.G. and Kurama, Y.C. (2004) A Friction Damper for Post-Tension Precast Concrete Beam-To-Column Joints. *13th World Conference on Earthquake Engineering*, Paper No.3189, Vancouver, B.C, Canada.
- Ricles, J.M., Sause, R., Peng, S.W. and Lu, L.W. (2002) Experimental evaluation of earthquake resistant post-tensioned steel connections. *Journal of Structural Engineering, ASCE*, 2002, 128:7, 850-859.
- Tsai, K-C., Chou, C-C, Lin, C-L., Chen, P-C. and Jhuang, S-J. (2008) Seismic self-centering steel beam-to-column moment connections using bolted friction devices. *Earthquake Engineering and Structural Dynamics*, 37, 627-645.
- Wolski, M., Ricles, J.M., Sause, R., and Lee, K.S. (2005) Energy dissipation for self-centering steel MRFs: bottom flange friction device. *US-Taiwan Workshop on Self-centering Structural System Report*, NCREE-05-004, Taipei, Taiwan.